CFD SIMULATION RESULTS FOR THE MINWATERCSP COOLING FAN

David VOLPONI [1], Tomasso BONANNI [1], Lorenzo TIEGHI [1], Giovanni DELIBRA [1], Alessandro CORSINI [1], Michael WILKINSON [2], Sybrand VAN DER SPUY [2], Theodor W. VON BACKSTRÖM [2]

[1] *Sapienza University of Rome, Dept. of Mechanical and Aerospace Engineering, Via Eudossiana 18, 00184 Roma, Italy*

[2] *Stellenbosch University, Department of Mechanical and Mechatronic Engineering, Joubert Street, Stellenbosch, 7600, South Africa*

SUMMARY

A 24 ft. diameter axial flow fan was developed for a hybrid cooling application, specifically aimed at concentrated solar power (CSP) plants. In order to evaluate its performance, the fan was modelled using Reynolds averaged Navier-Stokes (RANS) Computational Fluid Dynamics (CFD). A 1.542 m scale model of the fan was subsequently tested and the results compared to numerically obtained data. A redesign of the original fan has been carried out and evaluated using CFD. The results of all fans are compared to each other and discussed in this paper. The comparison shows that both fans have a maximum fan static efficiency in excess of 60 %. The results are also shown to correlate well with experimental results, which serves to verify the accuracy of the results.

INTRODUCTION

The MinWaterCSP project was initiated to develop methods for reducing the water consumption of concentrated solar power (CSP) plants. CSP plants are usually constructed in arid regions and as such water availability becomes one of the constraints on the viability of these plants. The majority of CSP plants (parabolic trough and central receiver) make use of a Rankine steam cycle to generate electricity. As part of the cycle the steam needs to be condensed and this is usually achieved by means of fan assisted wet cooled systems.

One solution to reducing the water consumption of wet cooling systems in power plants is to switch to dry-cooling. However, the water savings brought about by the use of dry-cooling are negated by the reduction in thermal efficiency of the power plant. This is caused by the increase in steam turbine back pressure associated with dry-cooling systems. The turbine back pressure becomes especially problematic under extreme climatic conditions such high temperatures and wind. The MinWaterCSP project proposes the use of a hybrid cooling system that is activated when the plant is exposed to these extreme conditions, in order to boost thermal performance. This hybrid cooling system will make use of large axial flow fans to drive air through the heat exchangers, condensing the process fluid [1].

A 24 ft. axial flow fan, referred to as the M-fan, was designed as part of the above project. This fan was specifically designed to meet the requirements of a relatively high flow rate and low pressure rise associated with current fin tube bundles used in dry-cooled systems [2]. In order to evaluate the newly designed fan it was modelled using computational fluid dynamics (CFD). The use of CFD to model large diameter axial flow fans has been shown by Augustyn [3] to deliver results that are within 4% of the values obtained from experimental tests of the same fans. The initial CFD results obtained in this manner are detailed in an earlier paper by Wilkinson et al. [4]. This publication shows a combination of design results, actuator disc and full 3-dimensional CFD results and verifies the accuracy of the design methods that were used. All computational domains were developed using ANSYS Workbench 17.2 and all simulations were performed using ANSYS FLUENT 17.2. As a further investigation, the M- and T-fans were also modelled in OpenFOAM [5]

To confirm the design of the M-fan, a 1.5 m diameter scale prototype was manufactured and tested in the ISO 5801 Part 1 Type A test facility at Stellenbosch University [6]. The test results were once again backed up by CFD simulation of the 1.5 m prototype. As a further investigation, an alternative fan design, referred to as the T-fan was developed with the purpose of reducing noise emissions and improving efficiency. CFD simulations of the 1.5 m diameter T-fan were performed, for comparison to the M-fan results. This paper gives an overview of the M- and T-fans, as well as their respective CFD simulation results. The paper concludes with a comparison of the performance of the M- and T-fans.

DETAILS OF THE M AND T-FANS

The development of the M-fan is detailed by Wilkinson et al. [4]. It was designed with an optimized hub-to-tip ratio based on the work of van Niekerk [7] and a velocity distribution that minimized the exit kinetic energy [8]. The resulting lay-out of the M-fan is shown in Figure 1.

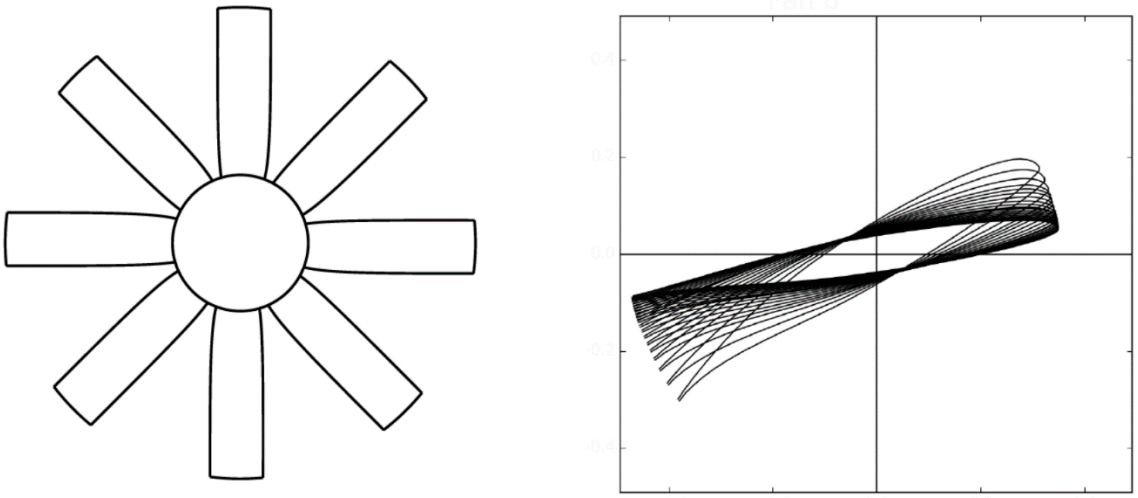

Figure 1- Schematic of the M-Fan (Left) and Stacking profile (Right) [4]

The design specification for the M-fan was obtained from the MinWaterCSP project. It was specified to be used as a large diameter cooling fan, to be a single rotor design and to have a diameter of 24 ft. The design results for the M-fan are summarised in Table 1.

Table 1 – M-Fan full scale characteristics [9]

Diameter	24 ft [7.3152 m]
Number of blades	8
Hub To Tip Ratio	0.29
Maximum Tip Gap	30 mm
Fan Rotational Speed	151 RPM
Flow Rate	333 m^3/s
Estimated Fan Static Pressure	116.7 Pa
Estimated Fan Shaft Power	63285.21 W
Estimated Fan Static Efficiency	61.4 %

The T-Fan was developed by re-staggering and adjusting the chord distribution of the M-Fan according to the Hybrid Design methodology, which is based on the coupling between the aerodynamic response of the selected blade profile and the vortex distribution [13]. The Hybrid design ensures a direct link between the load distribution on the blade and the profile performance. The aerodynamic characterisation (in terms of lift and drag coefficient) of each blade section defines the proper deflection capability [12] as is shown in Figure 2. Coupling the blade deflection capability with the target specific work distribution, the target angle of attack is automatically defined. Finally, the pitch distribution is computed using simple geometric consideration (see figure 3). With the purpose of reducing the anticipated noise emissions of M-Fan, the power law vortex distribution was selected. The near free vortex design postulated by Lewis [15] presents swirl velocities and thus blade loadings which taper rapidly to zero in the hub blade region. The unloading of the hub section reduces the possibility of recirculation in this zone especially at low flow rates improving global flow field stability and thus reducing noise emissions.

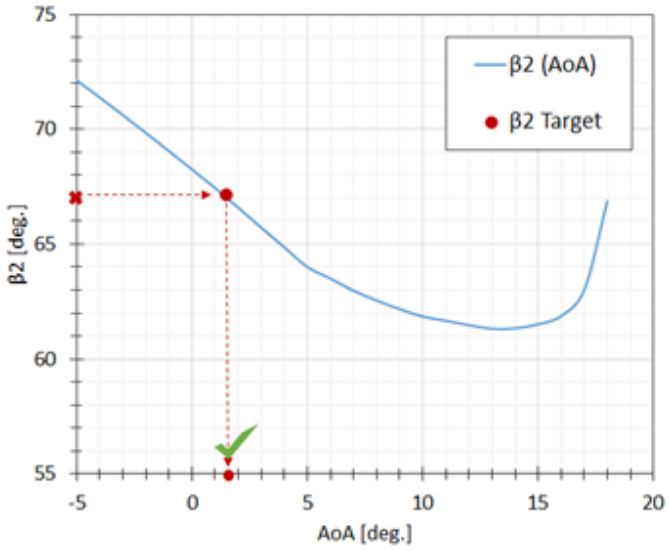

Figure 2: Mellor Chart

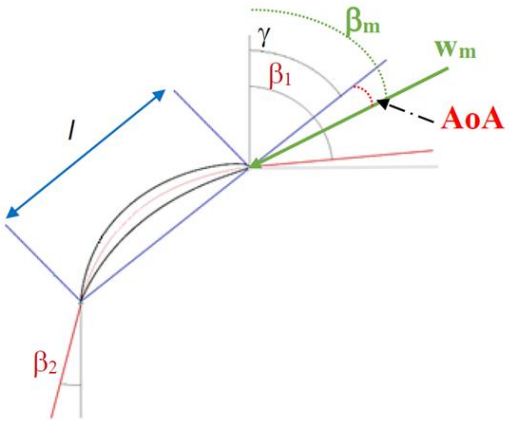

Figure 3: Blade geometrical parameterization

A comparison of the two designs in terms of chord length (c*) and twist is shown in Figure 4,where twist is defined as the change in angle from the intialblade setting angle.

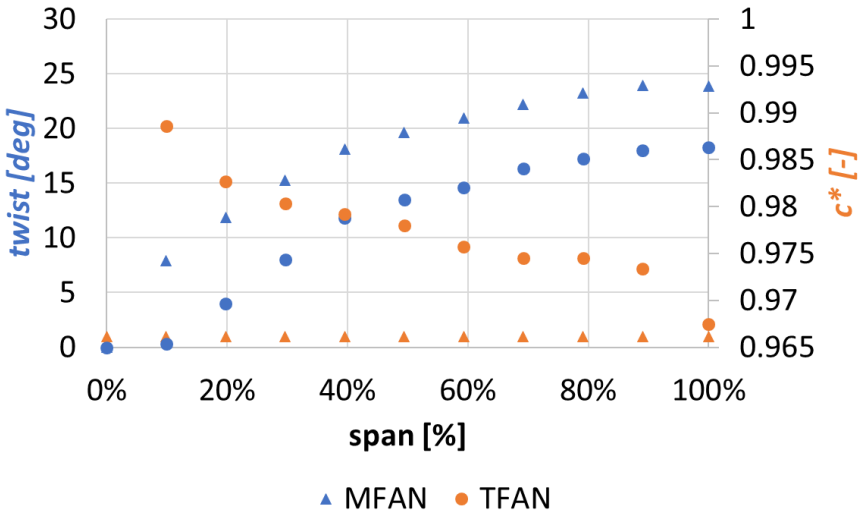

Figure 4: Comparison of M and T-fan stagger and chord.

ACTUATOR DISC MODELLING OF THE M-FAN

To evaluate the predicted outlet velocity profile of the designed fan the results from an actuator disc model (ADM) CFD simulation of the M-fan were also evaluated [4]. The ADM made use of aerofoil polar data derived from Xfoil [10]. The results from Xfoil were used to model the profiles of the M-fan, taking into account aerofoil camber variation and Reynolds number distribution in the fan.

The ADM makes use of blade element theory to calculate the momentum components introduced into the flow field by a fan rotor. Each fan blade is represented by discrete radial elements corresponding to the computational mesh seeding specified for the annular space of the fan in the radial direction. The lift and drag forces for the blade elements are incorporated into the Navier-Stokes equations of the CFD model as momentum source terms. The values for the lift and drag forces are calculated as follows:

$$\delta_L = \frac{1}{2}\rho|W_\infty|^2 C_L \times c \times \delta r \qquad (1)$$

$$\delta_D = \frac{1}{2}\rho|W_\infty|^2 C_D \times c \times \delta r \qquad (2)$$

Once the lift and drag forces were known the axial and tangential forces actuated by the fan blade element could be calculated. The effect of a discrete radial blade element is multiplied by the number of individual blades and then distributed equally along the circumference at a specific radius.

In the actuator disc, the fan blades are replaced with an annular disc, one cell wide, at the fan rotor plane (see Figure 5). A user defined function (UDF) is implemented at the fan rotor plane in order to introduce the relevant momentum source terms at the cells in the rotor disc. The momentum source terms are based on the average conditions obtained from the correpsonding up- and downstream discs, relative to the rotor disc. All three disks are made up of hexahedral mesh elements with identical cell distributions in the radial and tangential directions.

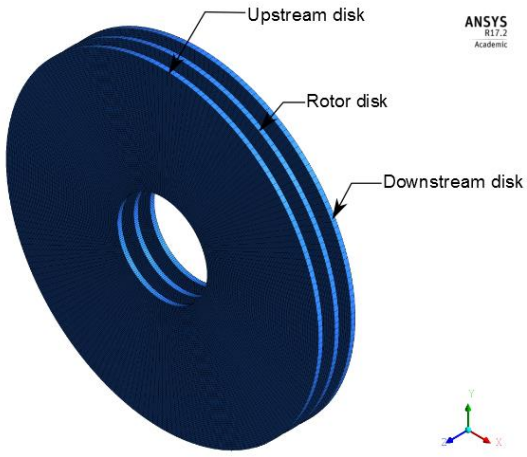

Figure 5: Lay-out of actuator disc model.

The average relative velocity vectors at the fan rotor were obtained from the up- and downstream discs. These vectors were then used to obtain the angle of attack across a fan blade element. This allowed the lift and drag forces generated by the blade to be calculated. Aerofoil lift and drag data, also commonly referred to as aerofoil polars were key to the implementation of the ADM, as mentioned in the previous section. The resultant lift and drag coefficients, obtained from Xfoil, are shown in Figure 6 as functions of radius ratio (RR) and angle of attack (α_{att}). Radius ratio is describe as the radius of any given blade section devided by the tip radius.

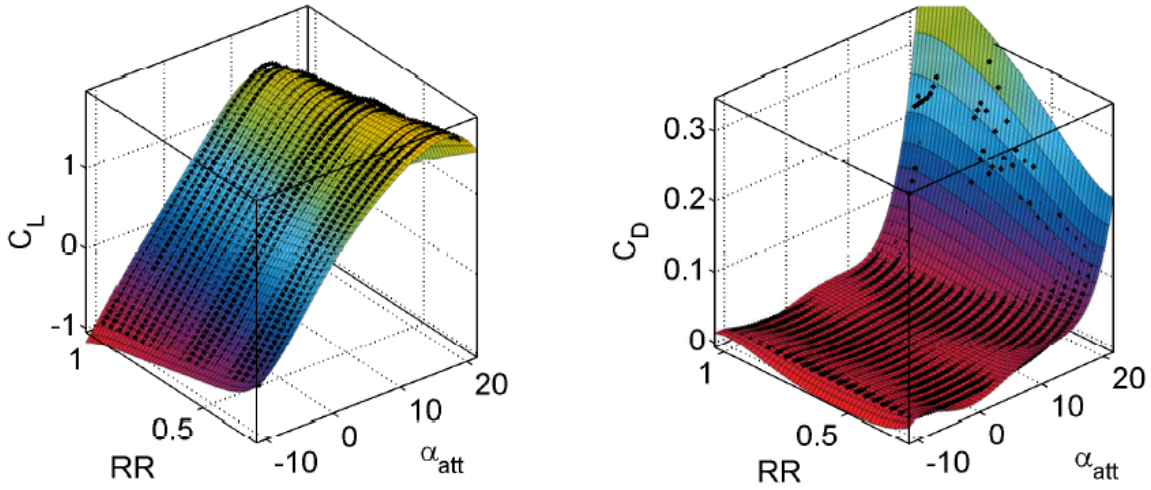

Figure 6: Spanwise lift and drag polars of the M-fan blading.

The computational domain used by the ADM is essentially a representation of the 1.5 m diameter ISO 5801 type A test fan test facility at Stellenbosch University, scaled up for a 24 ft. diameter fan. The domain and relevant boundary conditions are shown in figure 7.

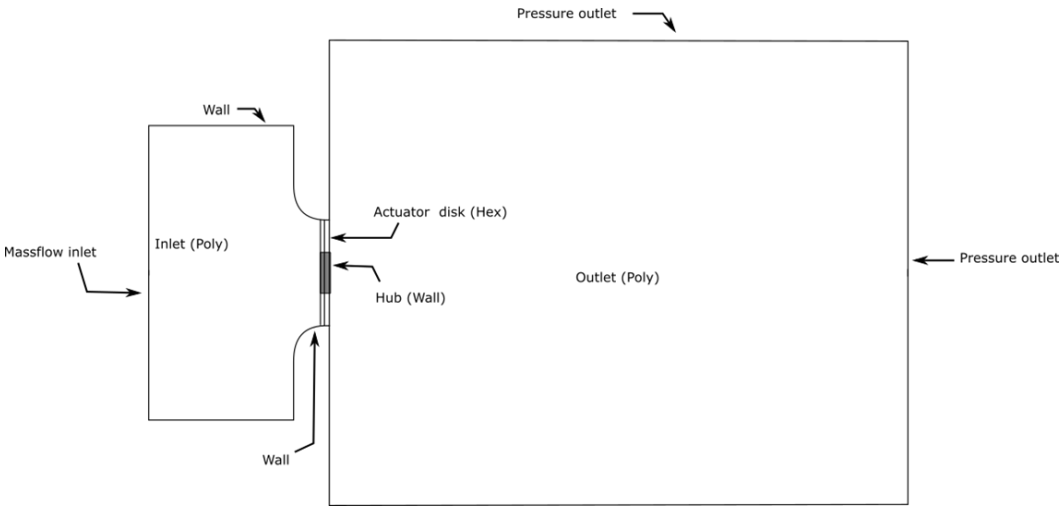

Figure 7: Computational domain for ADM.

The domain consisted of three sub-domains, the inlet, disc section and outlet. The inlet and outlet sub-domains consisted entirely out of polyhedral elements while the disks were made up of hexahedral elements. All walls had inflation applied in order to ensure that y+ values are in the range required by the selected k-ε realizable turbulence model ($30 < y+ < 300$). The mass flow inlet was specified to have a desired flow rate in the axial direction with a turbulence intensity of 3% and a length scale of 0.01. The pressure outlet boundaries were specified to have a gauge pressure of 0 Pa. The final mesh consisted of 3.1×10^6 cells, with 70 radial increments and 200 tangential increments in the three disks.

The realizable k-ε turbulence model of Shih et al. [11] with standard wall functions was applied for the ADM. This model has been shown to give results that correlate well with experimental fan test data [4].

NUMERICAL MODELLING (P3DM) OF M-FAN AND T-FAN

In order to validate the designs of the M and T-fans accurate numerical models of the fans were required. The process was started by modelling the M-fan in 24 ft. format, so that the results could be compared directly with the design values and ADM results. This was followed by a numerical model of the M-fan in 1.542 m diameter, in order to serve as a comparative link between the 24 ft. numerical results and 1.542 m ISO 5801 Type A test facility experimental results. Finally the T-fan was modelled in 1.542 m diameter format, in anticipation of future experimental work.

For all CFD analyses a one eighth segment containing a single blade was modelled. The P3DM computational domain consisted of three elements, the rotor subdomain and the upstream and downstream sub-domains. The construction of the overall domain for the 24 ft fan as well as relevant mesh boundary conditions is shown in Figure 8, along with the details of the rotor domain. The 1.5 m computational domain is identical in configuration to the 24 ft domain. The domain is orientated such that the negative z direction is the positive axial flow direction. The 24 ft fan is modelled with no tip gap, as well as a tip gap of 30 mm whereas the 1.5 m fan is modelled with a no tip gap and a 2 mm tip gap.

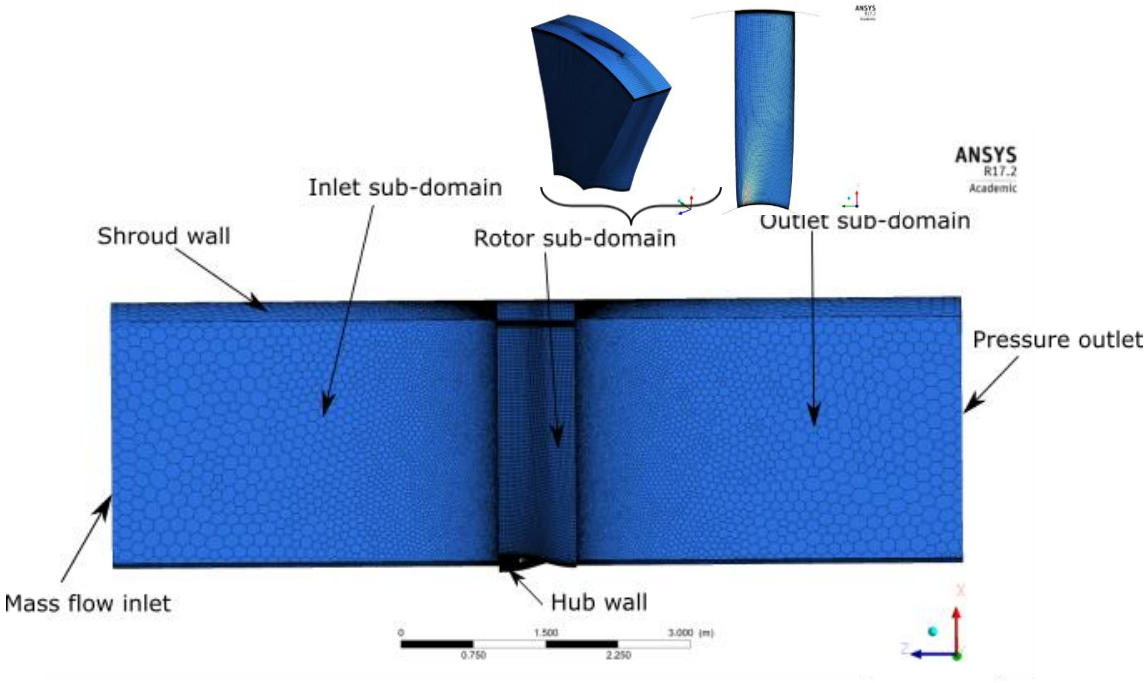

Figure 8: Computational domain for P3DM analyses.

The meshing of the blade passage was performed using ANSYS TURBOGRID. The mesh topology had been manipulated to ensure reasonable quality as well as ensuring that the majority of the elements are aligned in the flow direction, in order to reduce numerical error. For the 1.542 m diameter M-fan, a mesh independence survey found the minimum number of elements required in the passage to be in the order of 5×10^5. With this in mind the simulation mesh was made up of 1.8×10^6 elements. The passage mesh was made up entirely of hexahedral elements with 220 divisions along the blade span, which were used as discrete points when calculating the fan power. A 1 m long polyhedral inlet duct and a 1 m long outlet duct were added to the passage domain. These regions effectively extended the fan annulus in order to move the inlet and outlet planes further from the blade passage as this was found to improve solution stability. The inlet domain adjoined the inlet of the passage domain by means of a periodic repeat interface, the outlet domain joining the passage outlet in a similar manner.

The inlet boundary condition was set to be a massflow inlet. The hub and blade were set to be stationary walls. The shroud was set to be a rotating wall in order to be stationary relative to the rotating domain and the outlet was set to be a pressure outlet with a gauge pressure of 0 Pa. The entire domain was specified to rotate at the fan rotational speed in order to represent a rotating blade.

For all the P3DM CFD simulation the realizable k-e turbulence model was used with enhanced wall functions. Values of y+ were between 0 and 5, which is considered acceptable for this approach. Turbulence intensity at the inlet was set to 3 % at the inlet with a viscosity ratio 0.01. Other solver settings are presented in Table 2.

In order to obtain convergence the model was first run with first order momentum and turbulence settings before being switched to the higher order schemes as the simulation neared convergence. Final convergence levels obtained were in the order of 10^{-4}.

Table 2 - CFD Solver settings

Pressure-Velocity Coupling	SIMPLE
Pressure	PRESTO!
Gradient	Least Squares Cell Based
Momentum	QUICK
Turbulent Kinetic Energy	QUICK
Turbulent Dissipation Rate	QUICK

NUMERICAL MODELLING (P3DM) USING OPENFOAM

Concurrent RANS computations were also carried out using the simpleFoam solver of the OpenFOAM 2.3.x library for CFD computations with the non-linear closure of Lien et al [16]. to further verify the performance of the fan and analyze the flow field in the blade-to-blade passage. The Generalized Algebraic Multi-Grid solver (GAMG) was used for pressure and *smoothSolver* for the other equations. Both simulations were carried out until a full convergence of the fields, with a convergence threshold of 10^{-8} and 10^{-6} for pressure and the other quantities respectively.

Each computational domain includes a single blade to blade passage, using *Arbitrary Mesh Interface* (AMI) periodic boundaries at the mid-pitch. Both domains extend 1 chord upstream and 1.5 downstream of the leading edge and the trailing edge of the blades. Grid sizes are similar (8.3M cells for the M-FAN and 9.3M for the T-FAN). Distance of the first cell from the solid walls was adjusted to obtain a $y^+ \approx 1$. Statistics for the grids are reported in Table [3] and [4]. The total number of cells per blade surface was set to 500 (250 for each side of the blade), and 270 cells were set along the blade span. Tip clearance regions have been discretized using 30 cells in the radial direction.

Table 3 - M-fan computational grid

	Minimum	*Maximum*	*Average*
Volume ratio	1	5.9	1.1
Aspect ratio	1	180	5
Skewness	0	0.69	0.07
Min. included angle	20.17	90	73.5
y^+	0.79	4.9	2.67

Table 4 - T-fan computational grid

	Minimum	*Maximum*	*Average*
Volume ratio	1	4.3	1.15
Aspect ratio	1	103	8.7
Skewness	0	0.53	0.06
Min. included angle	30.5	90	73
y^+	0.67	4.6	2.34

The specified mass flow of the simulations was obtained by specifying a proper axial velocity profile at the inflow, with a turbulence level of 5 %. Lower (hub) and upper (shroud) endwall velocities were set to the proper rotational speed and to zero respectively. Near wall modelling of k and ε relied on OpenFoam kLowReWallFunction and epsilonLowReWallFunction. Convective boundary conditions were applied at the outlet.

RESULTS AND DISCUSSION

24 ft. M and T-fan numerical results

The 24 ft P3DM CFD results for the M-fan obtained using FLUENT are compared to the OpenFOAM results for the 24 ft M and T-fans as well as the actuator disk model results in figure 9. All P3DM simulations are run with the design tip gap of 30 mm. It can be seen that the ADM, FLUENT P3DM and OpenFOAM results indicate that the M-fan will not realise the desired design point pressure rise. The T-fan is shown to exceed the design point by 13.5%, although there is some uncertainty surounding this data point as it deviates from the expected performance trend. The OpenFOAM simulation of the M-fan predicts a pressure rise of 114.5 Pa at the operating point, whereas the FLUENT simulation predicts a pressure rise of 91 Pa. Based on the results of the ADM and OpenFOAM simulations the M-fan apprears to perform satisfactorily, however the P3DM results cast doubt on this and experimental validation is require. The T-fan appears to exceed the design point and would thus likely operate at a higher flow rate than 333 m^3/s in the heat exchanger system under normal operation.

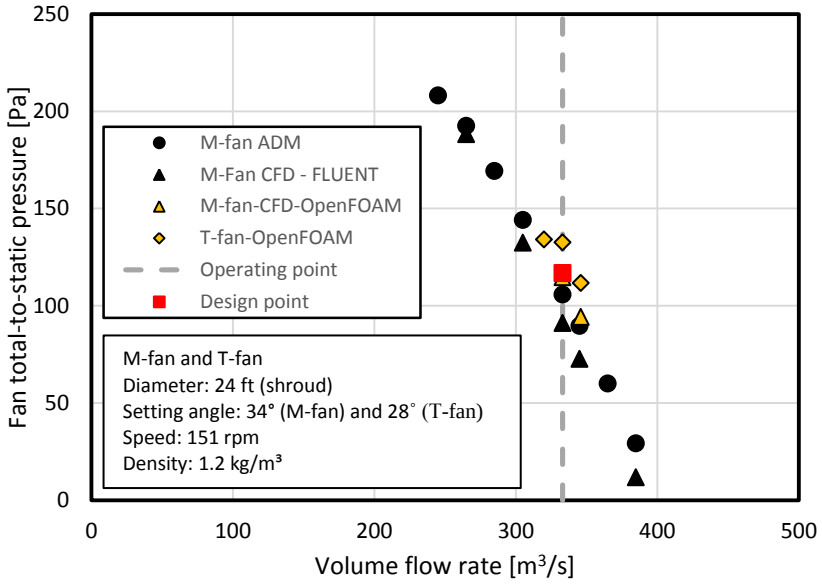

Figure 9: CFD estimated fan total-to-static pressure characteristics for the 24ft M and T-fans

Considering the fan total-to-static efficiency characteristics (Figure 10), the OpenFOAM results indicate the the T-fan will operate with an efficiency of 59% compared to the M-fan efficiency of 58 %. The ADM simulation indicates the most optimistic operating point efficiency of all the simulations. The FLUENT P3DM results for the M-fan indicate an operating point efficiency of 51 %, a lot lower than that predicted by the OpenFOAM simulations. These results indicate that the T-fan does provide a modest improvement on the M-fan in terms of efficiency. There is however a large degree of uncertainty in the data as is evident in the spread of efficiencies obtained at any point by the various simulations.

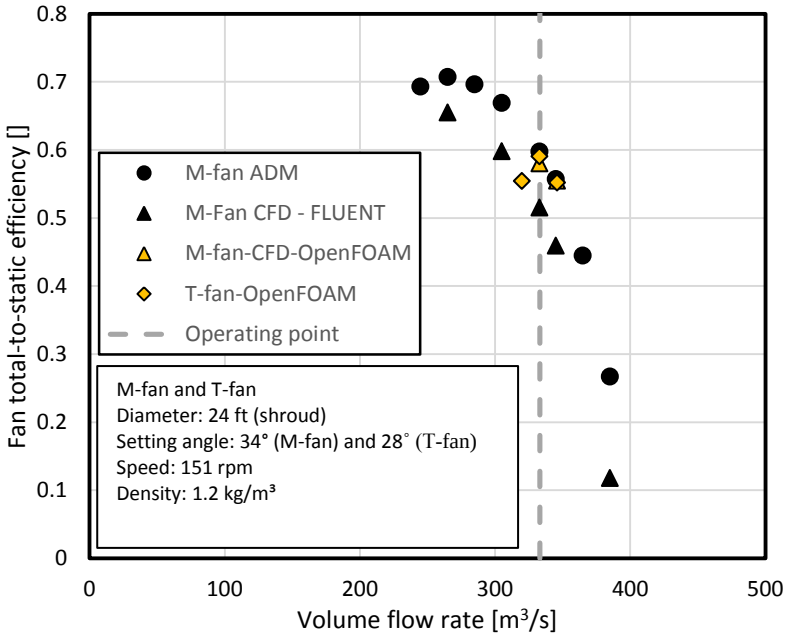

Figure 10: CFD estimated fan total-to-static efficiency characteristics for the 24 ft M and T-fans

1.5 m M and T-fan numerical results

In order to provide a greater degree of certainty the M and T-fans are simulated in Fluent at the 1.542 m diameter scale in identical compuational domains, in both cases with a 2 mm tip gap. These results are compared to experimentally obtained data for the M-fan operating under the same conditions.

The fan total-to-static pressure characteristics shown in figure 11 demonstrate that there is an excellent correlation between the CFD results for the M-fan and the experimental data. This validates the numerical techniques used to model both the M and T-fans. The data indicates that neither fan will meet the required pressure rise at the operating point, however the T-fan does provide a modest gain in performance over the M-fan in this regard. The T-fan is estimated to provide a fan total-to-static pressure of 108 Pa compared to 101 Pa for the M-fan. This provides a degree of certainty to the 24 ft results discussed previously where a similar improvement in pressure performance was shown for the T-fan. Further, this result indicates that the redesign performed to create the T-fan is based on valid assumptions and does indeed improve fan performance.

The results for the 1.5 m fans in terms of fan total-to-static efficiency are shown in figure 12. Once again there is good corelation between the experimental and numerical data for the M-fan, however the numerical results tend to underestimate efficiency by approimately 6 % at the operating point. These results indicate that the T-fan has a modestly improved fan total-to-static efficiency at the opperating point when compared to the M-fan, a gain of approximately 2 %. This indicates that the T-fan design is successful and provides an improvement in performance compared to the M-fan. The experimental validation of the modelling technique adds an improved degree of certainty to this result.

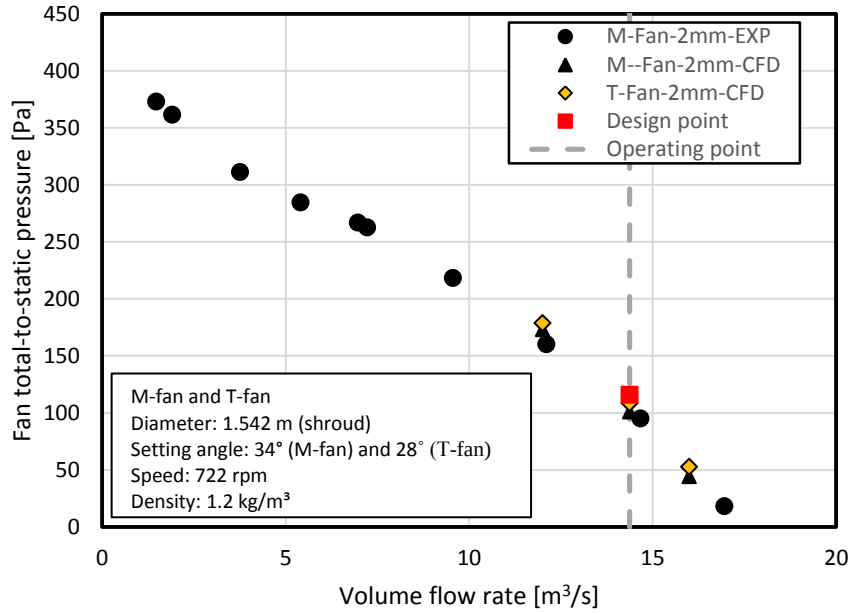

Figure 11:Fan total-to-static pressure characteristics for the 1.5 m M and T-fans

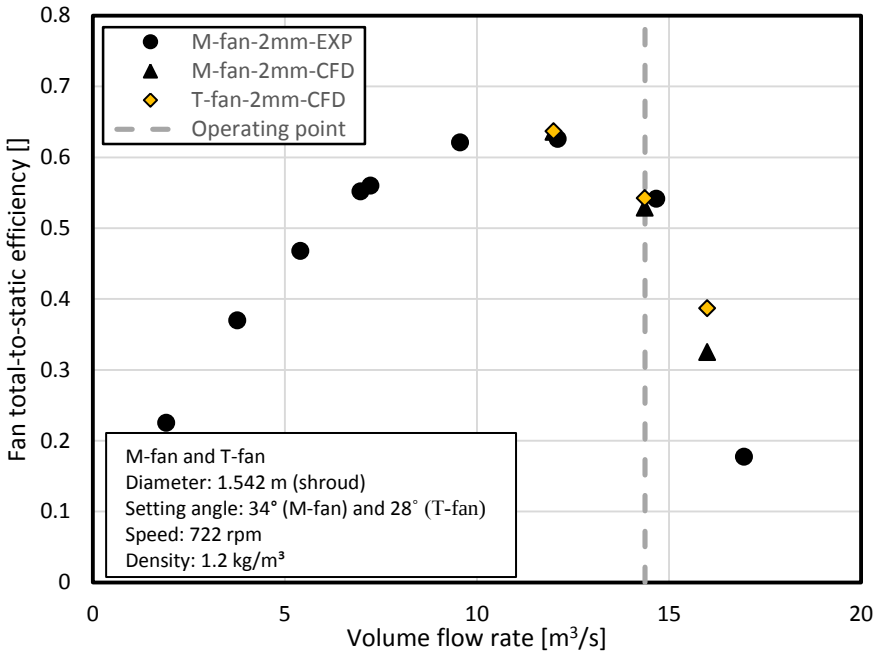

Figure 12: Fan total-to-static pressure characteristics for the 24ft M and T-fans

In order to provide further insight into the differences between the M-fan and T-fan, flow field data is extracted half a chord length downstream of the fans for the CFD simulations of the operating point. These results are presented in terms of absolute axial and tangential velocity distributions in figures 13 and 14. In terms of axial velocity the distributions are near identical for the upper two thirds of the blade span, however the outlet axial velocity predicted for the T-fan is higher than that of the M-fan. This is in line with the design method followed for the T-fan which aimed to unload the blade root. In terms of tangential velocity , as shown in figure 14, the T-fan has an increased exit tangential velocity compared to the M-fan, esspecialy nearer the blade root. This explains the improvement in fan total-to-static pressure performance of the T-fan over the M-fan, as according to Lewis [15] the exit tangential velocity at a rotor exit is associated with the pressure rise provided by that rotor. This result demonstrates the effectiveness of the Hybrid Method used to design the T-fan as the flow field has been altered in a way that reduces blade twist at the root while improving the flow turning across the entire blade span.

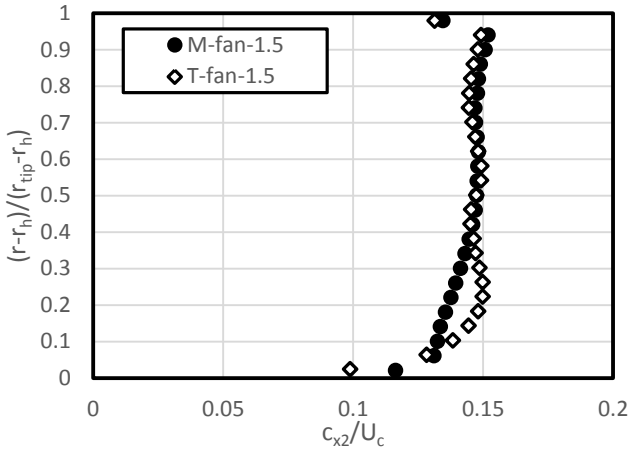

Figure 13: Exit axial velocity profiles for the M and T-fans

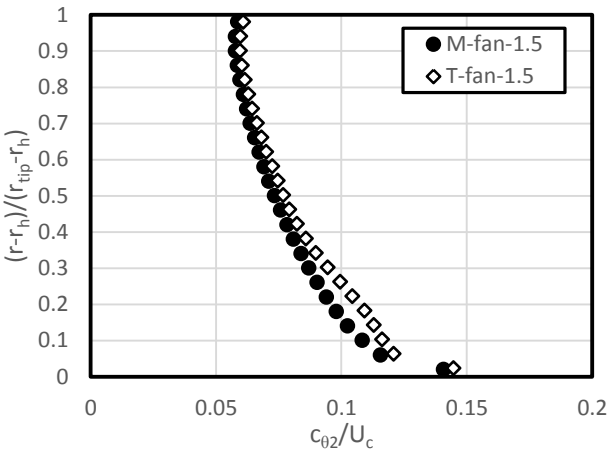

Figure 14: Exit tangential velocity profiles for the M and T-fan

CONCLUSIONS

Two fan designs for a hybrid cooling application have been compared at two different scales using a variety of numerical models. The M-fan design is shown to under perform in terms of pressure rise at both the 24 ft and 1.5 m scales. The T-fan which is a redesign of the M-fan is shown to provide improved performance in terms of both pressure and efficiency. This indicates that the method used to design the T-fan is valid and provides a remedy to the performance issues entountered with the M-fan.

Further simulations performed at 1.5 m scale for the M-fan are validated against experiemental data, providing confidence in the numerical methods used in this study as well as findings made. CFD simulations of the T-fan indicate the it will provide a 2 % improvement in fan total-to-static efficiency at the operating point, as well as providing an improvement in total-to-static pressure rise when compared to the M-fan. A comparison of the blade exit flow fields of the M-fan and T-fan at 1.5 m scale provide further validation to the Hybrid Method used to design the T-fan. The unloading of the blade root and redistribution of specific work across the blade span are shown to increase flow turning, while reducing blade twist.

Future work planned based on the outcomes of this study includes experimental testing of the 1.5 m T-fan as well as an experimental comparison of the M and T-fan exit flow fields in order to futher validate the T-fan design, as well as the CFD results.

ACKNOWLEDGEMENTS

The financial assistance of the National Research Foundation (NRF) towards this research is hereby acknowledged. Opinions expressed and conclusions arrived at, are those of the author and are not necessarily to be attributed to the NRF.

This project has received funding from the European Union's Horizon 2020 research and innovation programme under grant agreement No. 654443

This communication related to the action MinWaterCSP is made by the beneficiaries and it reflects only the author's view. The European Commission is not responsible for any use that may be made of the information it contains.

Computations were performed using the University of Stellenbosch's Rhasatsha HPC: http://www.sun.ac.za/hpc.

BIBLIOGRAPHY

[1] The MinWaterCSP Project - http://www.minwatercsp.eu/minwatercsp_project/ **2017**

[2] Bruneau, P. R. P. – *The design of a single rotor axial flow fan for a cooling tower application*. M Eng. Thesis. Stellenbosch University. **1994**

[3] van der Spuy, S. J., von Backström, T.W. – *Performance of rotor-only axial fans designed for minimum exit kinetic energy*. R&D Journal, Volume 18 (3). **2002**

[4] Wilkinson, M.B., van der Spuy, S. J., von Backström, T.W. – *The Design of a Large Diameter Axial Flow Fan for Air-Cooled Heat Exchanger Applications*. ASME Turbo Expo 2017: Turbomachinery Technical Conference and Exposition. American Society of Mechanical Engineers, p. V001T09A002-V001T09A002. **2017**

[5] H. G. Weller, G. Tabor, H. Jasak, C. Fureby, A tensorial approach to computational continuum mechanics using object-oriented techniques, COMPUTERS IN PHYSICS, VOL. 12, NO. 6, NOV/DEC 1998.

[6] ISO 5801: 2007 – *Industrial Fan – Performance Testing using Standardised Airways.* **2007**

[7] van Rossum, G., Drake, F.L. - *The Python Language Reference Manual.* Network Theory Ltd. **2011**

[8] Drela, M. - *Xfoil: An analysis and design system for low Reynolds number airfoils.* Low Reynolds number aerodynamics, pp. 1_12. **1989**

[9] Vanderplaats, G.N. - *Development of a Flexible Optimization Capability*. Vanderplaats R&D Inc, Colorado Springs, Colorado, USA. **1999**

[10] Louw, F.G. – *Investigation of the Flow Field in the Vicinity of an Axial Flow Fan during Low Flow Rates.* PhD. Thesis, Stellenbosch University. **2015**

[11] Ströhmaier, C.K. – *An Evaluation of a Scale Model Medium Speed Wind Tunnel.* M Eng. Thesis, Stellenbosch University. **1996**

[12] Kirstein, C.F., von Backström, T.W. – *Flow through a solar chimney power plant collector-to-chimney transition section.* Journal of Solar Energy Engineering, 128.3: 312-317. **2006**

[13] Bonanni T.,Bublitz M., Corsini A., Delibra G., Sheard A. G., Volponi D., (2017), 'Design of a Single Stage Variable Pitch Axial Fan', *GT2017-64517*

[14] Mellor, G., (1957), 'The aerodynamic Performance of Axial Compressor Cascades with Applications to Machine Design', (sc.D.Thesis), *M.I.T. Gas Turbine Lab, M.I.T. Rep. No. 38.*

[15] R. I. Lewis, (1996), 'Turbomachinery performance Analysis', *Butterworth-Hainemann*

[16] Lien, F. S., Kalitzin, G., & Durbin, P. A. (1998). RANS modeling for compressible and transitional flows. *Proceedings of the Stanford University Center for Turbulence Research Summer Program*, 267-286.